Reaction Kinetics and Thermodynamic Modeling of Sodium Hydroxide Activated Slag Paste

Zuo, Yibing; Nedeljkovic, Marija; Ye, Guang

Publication date
2016

Document Version
Accepted author manuscript

Published in
3rd International RILEM Conference on Microstructure Related Durability of Cementitious Composites

Citation (APA)
Zuo, Y., Nedeljkovic, M., & Ye, G. (2016). Reaction Kinetics and Thermodynamic Modeling of Sodium Hydroxide Activated Slag Paste. In C. Miao, W. Sun, J. Liu, H. Chen, G. Ye, & K. van Breugel (Eds.), *3rd International RILEM Conference on Microstructure Related Durability of Cementitious Composites: Nanjing, China* (Vol. 117, pp. 1-8). RILEM Publications S.A.R.L..

Reaction Kinetics and Thermodynamic Modeling of Sodium Hydroxide Activated Slag Paste

Yibing Zuo (1), Marija Nedeljkovic (1) and Guang Ye (1)

(1) Materials and Environment (Microlab), Faculty of Civil Engineering and Geosciences, Delft University of Technology, The Netherlands

Abstract

The technology of alkaline activation of calcium aluminosilicate materials, as an alternative to Portland cement to produce a clinker-free material, can address the energy and environmental concerns associated with Portland cement production. As this technology attracts more and more attention in recent years, there are increasing researches carried out on the thermodynamics of alkali-activated slag cement. However, none of the thermodynamic modeling studies were carried out in combination with the reaction kinetics of alkali-activated slag. As a result, the modeling results were expressed in term of reaction extent instead of time, which makes it difficult and inconvenient to compare with the experimental results that are usually indicated as a function of time. In order to deal with this issue in this study, the reaction kinetics of sodium hydroxide activated slag (SHAS) was studied through the measurement of heat evolution rate and quantified as a function of time using the modified Jander equation. The quantification of reaction kinetics enables the correlation between the reaction extent and time, by which the hydration of SHAS can be thermodynamically simulated in a time scale. The simulated elemental concentrations in the aqueous solution show a good agreement with the experimental results in the altering trend, and match the experimentally measured solubility data to be within ±1 order of magnitude. The phase assemblages of SHAS simulated as a function of time using thermodynamic modeling, shows no obvious dependence on the Na_2O content in the range of 4% to 8%. Based on the modeled phase assemblages, some properties can be calculated as a function of time, such as chemical shrinkage, capillary porosity, etc.

Keywords: Reaction kinetics, Thermodynamic modeling, Sodium hydroxide, Slag, Quantification

1. INTRODUCTION

Thermodynamics has been playing an essential role in the understanding of chemical reactions. It can predict whether a reaction can happen and to calculate the stable phase assemblage and the aqueous phase composition at the final state once the reaction is completed. As an application of thermodynamics, the thermodynamic modeling has been extensively and successfully used in the research of hydration in Portland cement-based materials [1]. However, the utilization of thermodynamic modeling was only introduced in recent years to study the hydration of alkali-activated slag due to the lacking model and insufficient solubility data on the primary reaction products.

Lothenbach and Gruskovnjak used a solid solution model to simulate the primary reaction products in the alkali-activated slag cement [2]. In this approach, the uptake of Al was considered using Al/Si ratio of 0.1 and the uptake of sodium was considered very roughly using a distribution ratio of sodium in primary reaction products relative to the sodium in the aqueous solution. However, for the thermodynamic modeling, the ability to formally account for the uptake of Al and Na into the primary reaction products is of great significance. Myers et al., for the first time, proposed a thermodynamic model to account explicitly for the structurally-incorporated Al and Na species in the primary reaction products, C-(N)-A-S-H gel, and apply it to simulate the chemistry of primary reaction products in alkali-activated slag cement [3]. Afterwards, many researches have been carried out on the hydration of alkali-activated slag materials using this model [4-6]. However, none of these thermodynamic modeling studies were carried out in combination with the reaction kinetics of alkali-activated slag. As a result, the modeling results were expressed in term of reaction extent instead of time, which makes it difficult and inconvenient to compare with the experimental results that are usually indicated as a function of time.

In order to deal with this gap between thermodynamic modeling results and experimental results, reaction kinetics of sodium hydroxide activated slag (SHAS) was studied through the measurement of heat evolution rate and quantified as a function of time using the modified Jander equation. The quantification of reaction kinetics enables the correlation between the reaction extent and time, by which the hydration of SHAS was thermodynamically simulated in a time scale.

2. MATERIALS AND METHODS

2.1 Materials and mixtures

The chemical composition of blast furnace slag tabulated in Table 1 was measured by X-ray fluorescence spectrometry (XRF). The activating solution was prepared through mixing sodium hydroxide (analytical grade, >98%) with distilled water. Three levels of sodium oxide content with respect to slag were selected (Na_2O/slag=4, 6 and 8 wt. %). The water to slag ratio in weight was fixed at 0.4 for all mixtures. According to the content of sodium oxide, the mixtures can be denoted as Na_2O_4%, Na_2O_6% and Na_2O_8% corresponding to the mixture with Na_2O/slag=4, 6 and 8% respectively.

Table 1: Chemical composition of blast furnace slag.

Oxide	SiO_2	CaO	Al_2O_3	MgO	Fe_2O_3	SO_3	K_2O	TiO_2	L.I.
Weight (%)	32.91	40.96	11.85	9.23	0.46	1.61	0.33	1.00	1.15

2.2 Reaction kinetics

Reaction kinetics were studied using isothermal conduction calorimetry in accordance with ASTM C1679 at 20 ℃. All the raw materials were conditioned at the measurement temperature of 20 ℃ to avoid any temperature difference. Alkaline solutions with the desired concentrations were prepared and allowed to cool to room temperature prior to mixture preparation. The mixture pastes were prepared by mixing slag and activating solution externally and immediately placed into the calorimeter (TAM-Air-314) at the temperature of 20 ℃. Two replicates were measured simultaneously. The heat flow was recorded and the cumulative heat was calculated up to one week.

2.3 Thermodynamic modeling

The newly developed thermodynamic approach by Myers et al [3] was adopted in this paper. The chemical reactions and corresponding solubility products of the eight end-members for the primary reaction products, C-(N-)A-S-H gel, and the three end-members for hydrotalcite-like phases were reproduced in [6]. Lothenbach and Gruskovnjak reported that mackinawite is more stable in the alkali-activated slag system than other phases like Fe-ettringite or microcrystalline $Fe(OH)_3$ [2]. Therefore mackinawite was included here to consider the reactions between aqueous Fe^{2+} and S^{2-} under ambient conditions. More details on the thermodynamic properties of other secondary reaction products can be referred to [4].

Simulations for the three mixtures were carried out in an N_2 atmosphere at 25 ℃, 1 bar using GEM-Selektor V3 (http://gems.web.psi.ch/) [7, 8]. Congruent slag dissolution was assumed and proportional additions of SiO_2, CaO, Al_2O_3, MgO, Fe_2O_3, H_2S and K_2O were used to simulate the slag reaction extents and bulk chemical composition. Usually the slag contains more than 95% vitreous phase [9]. Considering the impurities of slag, this study takes SiO_2, CaO, Al_2O_3, MgO, Fe_2O_3, H_2S and K_2O to be fully dissolved and reacted in the modeling. It is worth noting that the samples were cured at 20 ℃ in experiments, which is slightly different from the standard equilibrium temperature. However, this difference does not have a significant influence on the rate of diffusion or the stability of minerals [10], and hence would not impose a significant impact on the equilibrium constants and the thermodynamic modeling results.

3. RESULTS AND DISCUSSION

3.1 Calorimetric response of SHAS pastes

Figure 1 presented the heat evolution rate and cumulative heat release over the testing period for the SHAS pastes. It can be seen that two calorimetric peaks could be readily observed from the heat evolution rate curves for all studied mixtures (Figure 1(A)), which agrees with the observations in [11, 12]. The first peak with significant high heat flow within the first 10 minutes corresponds to the dissolution/wetting of slag after mixing with alkaline solutions [11]. The second peak occurred between 1 h and 3 h is assigned to the formation of large amounts of reaction products [13]. According to those two calorimetric peaks, the entire hydration process of SHAS can be divided into three reaction stages, namely initial dissolution, acceleration/deceleration and stable period. In comparison with the four distinctive reaction stages (dissolution, dormant, acceleration/deceleration and steady state) in hydration of a normal Portland cement, no noticeable induction period was observed in the hydration process of SHAS pastes.

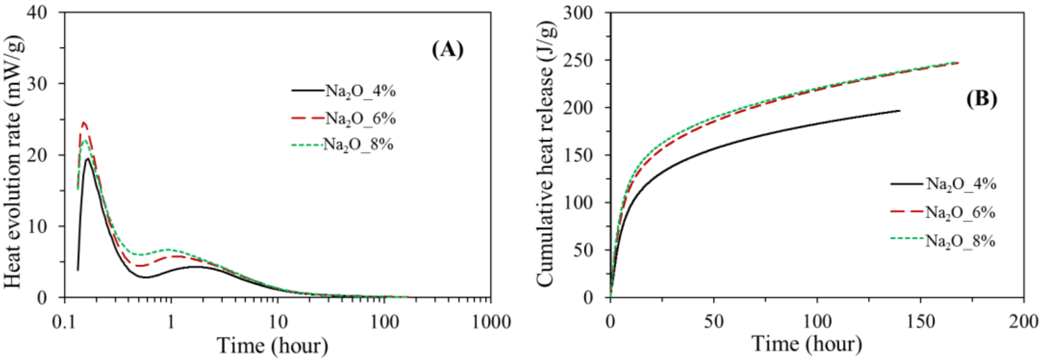

Figure 1: Heat evolution rate (A) and cumulative heat release (B) for SHAS pastes

The cumulative heat release curves for SHAS pastes (Figure 1(B)) indicates more heat release with increasing sodium oxide content. However, higher addition of sodium oxide does not show an obvious influence as regards increasing the cumulative heat release after sodium oxide content reaches 6%.

3.2 Quantification of reaction kinetics of SHAS

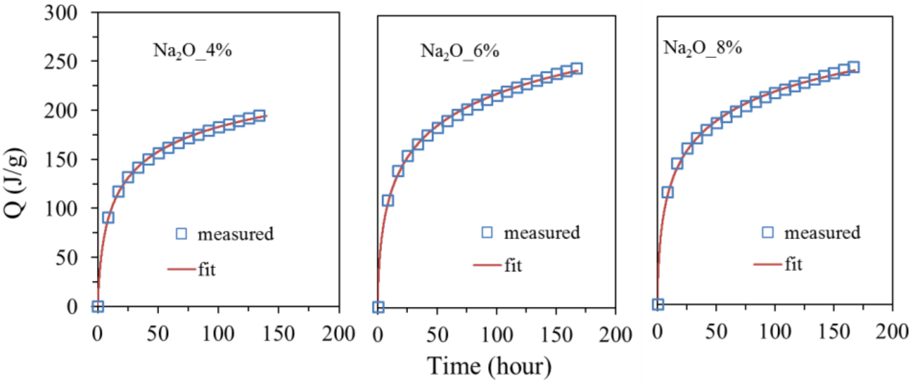

Figure 2: Exponential fits applied to the cumulative heat release for SHAS pastes. Symbols represent the experimental data points (1 out of 1000 shown) and the solid lines show the fit of Eq. (2) to the experimental data.

The time-dependent degree of slag reaction (α(*t*)) can be calculated as a ratio of cumulative heat release at time *t* (Q(*t*)) to the total heat release (Q_{max}).

$$\alpha(\mathrm{t}) = \frac{\mathrm{Q(t)}}{\mathrm{Q_{max}}} \tag{1}$$

The cumulative heat release at time *t*, Q(*t*), was obtained by integrating the heat evolution rate curves (Figure 1(A)) and shown in Figure 1(B). In order to obtain the total heat release, Q_{max}, an exponential model was used [11, 14].

$$Q(t) = Q_{max}\exp(-\left[\frac{\tau}{t}\right]^{\beta}) \tag{2}$$

Where, τ and β are the time parameter and the shape parameter respectively. Fits of the Q(*t*) vs. *t* curves for the SHAS pastes was shown in Figure 2. The fitted curves match well with the experimental relationship curves, indicating that Eq. (2) can well characterize the cumulative heat release as a function of time.

The total heat release and fitted parameters were listed in Table 2. Among the SHAS mixtures, the mixture with 6% of sodium oxide with respect to slag (Na_2O_6%) has the largest amount of total heat release. Given the total heat release, the degree of slag reaction can be calculated according to Eq. (1).

Table 2: Total heat release and fitted parameters of the exponential model

Samples	Q_{max} (J/g)	τ	β
Na_2O_4%	319.5	17.94	0.34
Na_2O_6%	520.3	54.91	0.25
Na_2O_8%	466.5	32.38	0.26

Since the modified Jander equation can model consecutive and sometimes overlapping reaction processes, it was used to characterize the degree of reaction of SHAS pastes as shown in Eq. (3) in its linear form [11, 15].

$$\ln\left[1-(1-\alpha(t))^{1/3}\right]=\frac{1}{N}\ln k_D+\frac{1}{N}\ln t \qquad (3)$$

Where k_D is the rate constant that implicitly accounts for the diffusion coefficient and the reaction grade N represents the rate controlling mechanisms. In order to determine the reaction grade N and rate constant k_D in Eq. (3), each part of $\ln[1-(1-\alpha(t))^{1/3}]$ *vs.* ln *t* curve was linearly regressed as shown in Figure 3.

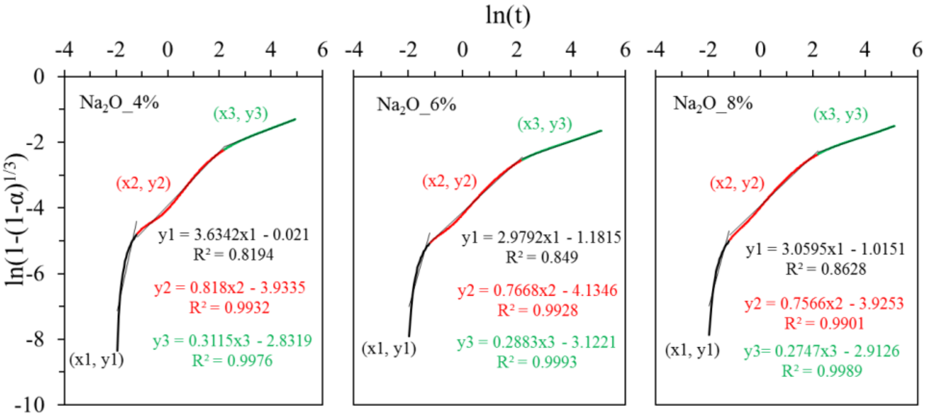

Figure 3: Linear fits applied to $\ln[1-(1-\alpha(t))^{1/3}]$ vs. ln *t* relationship for pure SHAS pastes.

The regressed equations show a very good linearity between ln[1-(1- α(t))1/3] and ln *t* in each reaction stage. Given the regressed equations for each reaction stage the reaction grade N and rate constant k_D were calculated and tabulated in Table 3. According to the reaction grade N, reaction in the three reaction stages (dissolution, acceleration/deceleration and stable period as indicated in Figure 1(A)) was governed by nucleation mechanism ($N<1$), phase-boundary mechanism ($N\approx1$) and the slowest transport process ($N>2$) respectively regardless of the sodium oxide content. Given the transition time, reaction grade and rate constant, the degree of slag reaction can be quantified as a function of time using Eq. (3).

Table 3: Transition time, reaction grade and rate constant

Sample	Transition time (h)		1^{st} reaction stage		2^{nd} reaction stage		3^{rd} reaction stage	
	t_1	t_2	N	k_D	N	k_D	N	k_D
Na_2O_4%	0.4	9	0.28	0.99	1.22	0.0082	3.21	0.00011
Na_2O_6%	0.4	9	0.34	0.67	1.3	0.0046	3.47	0.000019
Na_2O_8%	0.5	9	0.33	0.72	1.32	0.0056	3.64	0.000024

3.3 Thermodynamic modeling in a time scale

Figure 4 presents the simulated concentrations of Na, OH^-, Al, Si and Ca in the aqueous phase composition as a function of time till complete hydration of slag using thermodynamic modeling (hereafter denoted as [Na], [OH^-], [Al], [Si] and [Ca]). It can be seen that [Na] and [OH^-] dominate the aqueous phase composition of pore solution in SHAS, increase with increase of Na_2O content from 4% to 8% and decrease gradually with elapse of time. [Ca] remains at a very low level and does not shown an obvious change, which is due to the low solubility of Ca in high alkalinity environment as indicated by the high [OH^-]. [Al] and [Si] decrease with time as they react to form reaction products. On the other hand, the Na_2O content increases [Al] and [Si] as high alkalinity accelerates the dissolution of slag.

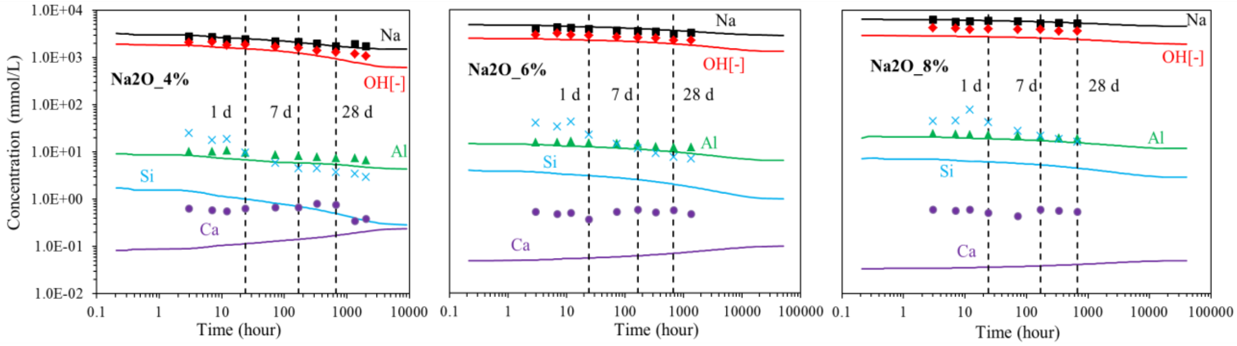

Figure 4: Pore solution chemical composition of SHAS (the curves are simulated by thermodynamic modeling and the symbol points are experimental data reported in a previous work [6]).

The simulated elemental concentrations show a good agreement with the experimental results in the altering trend as a function of time. Regarding to the magnitude, the simulated solubility results match the experimentally measured solubility data to be within ±1 order of magnitude as shown in Figure 5. The poor agreements were found for [Si] and [Ca] that were underestimated by the thermodynamic modeling.

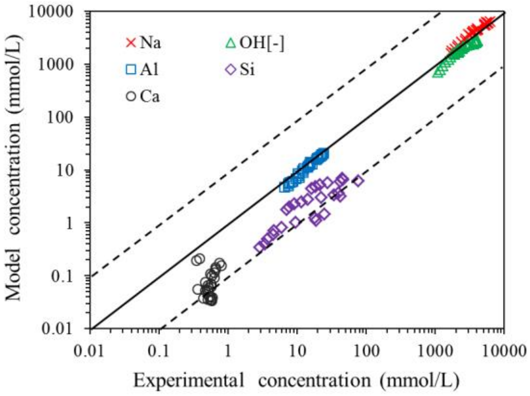

Figure 5: Simulated elemental concentrations in the aqueous phase compared to experimental pore solution composition for SHAS pastes [6].

The phase assemblages of SHAS can also be simulated as a function of time till complete hydration of slag using thermodynamic modeling as presented in Figure 6. It can be seen that Na_2O content in the range of 4% to 8% does not impose much influence on the phase assemblage while influences only a little bit on the formation of portlandite. In the mixture with 4% of Na_2O content, only trace amount of portlandite was formed before 7 d, while for the other two mixtures, production of portlandite increases with elapse of time. Based on the thermodynamic modeled phase assemblages, some properties can be calculated as a function of time, such as chemical shrinkage, capillary porosity, the volume ratio between reaction products and reacted slag, etc., which enables convenient and direct comparisons with the experimental results that are usually expressed in a time scale.

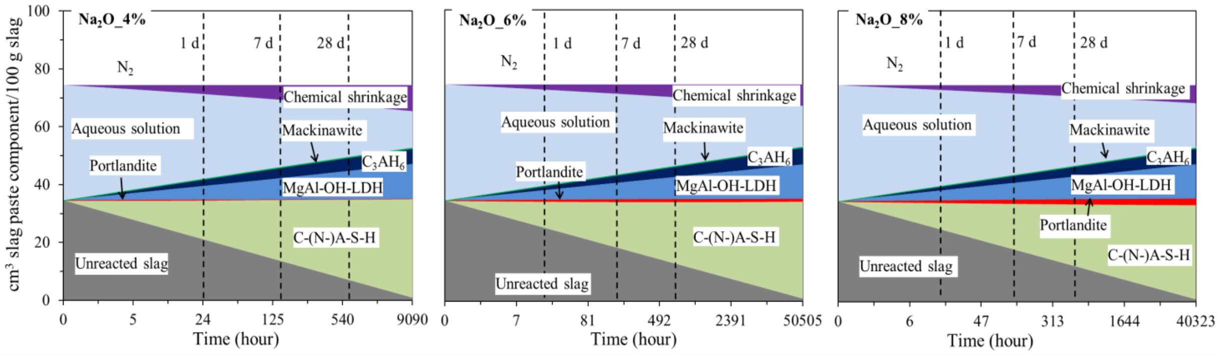

Figure 6: Simulated phase assemblages as a function of time

4. CONCLUSIONS

(1) The reaction kinetics of SHAS were quantified using the modified Jander equation. The reaction in the three successive reaction stages (dissolution, acceleration/deceleration and stable period) was governed by nucleation mechanism ($N<1$), phase-boundary mechanism ($N\approx1$) and the slowest transport process ($N>2$) respectively regardless of the sodium oxide content from 4% to 8%.

(2) The elemental concentrations as a function of time were simulated through thermodynamic modeling. The simulated elemental concentrations show a good agreement

with the experimental results in the changing trend, and match the experimentally measured solubility data to be within ±1 order of magnitude.

(3) The phase assemblages of SHAS were simulated as a function of time using thermodynamic modeling, showing no obvious dependence on the Na_2O content in the range of 4% to 8%. Based on the modeled phase assemblages, some properties can be calculated as a function of time, such as chemical shrinkage, capillary porosity, etc.

ACKNOWLEDGEMENTS

Microlab at TU Delft is appreciated and YZ thank the China Scholarship Council (CSC).

REFERENCES

[1] Damidot, D., Lothenbach, B., Herfort, D. and Glasser, F. P., 'Thermodynamics and cement science', *Cement and Concrete Research* **41** (7) (2011) 679-695

[2] Lothenbach, B. and Gruskovnjak, A., 'Hydration of alkali-activated slag: thermodynamic modelling', *Advances in cement research* **19** (2) (2007) 81-92

[3] Myers, R. J., Bernal, S. A. and Provis, J. L., 'A thermodynamic model for C-(N-)A-S-H gel: CNASH-ss. Derivation and validation', *Cement and Concrete Research* **66** (2014) 27-47

[4] Myers, R. J., Lothenbach, B., Bernal, S. A. and Provis, J. L., 'Thermodynamic modelling of alkali-activated slag cements', *Applied Geochemistry* **61** (2015) 233-247

[5] Ye, H. and Radlińska, A., 'Quantitative Analysis of Phase Assemblage and Chemical Shrinkage of Alkali-Activated Slag', *Journal of Advanced Concrete Technology* **14** (5) (2016) 245-260

[6] Zuo, Y., Nedeljkovic, M., Arbi, K. and Ye, G., 'Thermodynamic modeling and experimental study of alkali-activated slag paste', in Proceedings of 4th International Symposium on Ultra-High Performance Concrete and High Performance Construction Materials, Kassel, March, 2016 25-26

[7] Kulik, D. A., Wagner, T., Dmytrieva, S. V., Kosakowski, G., Hingerl, F. F., Chudnenko, K. V. and Berner, U. R., 'GEM-Selektor geochemical modeling package: revised algorithm and GEMS3K numerical kernel for coupled simulation codes', *Computational Geosciences* **17** (1) (2013) 1-24

[8] Wagner, T., Kulik, D. A., Hingerl, F. F. and Dmytrieva, S. V., 'GEM-Selektor geochemical modeling package: TSolMod library and data interface for multicomponent phase models', *The Canadian Mineralogist* **50** (5) (2012) 1173-1195

[9] Chen, W. and Brouwers, H., 'The hydration of slag, part 1: reaction models for alkali-activated slag', *Journal of materials science* **42** (2) (2007) 428-443

[10] Lothenbach, B., Matschei, T., Möschner, G. and Glasser, F. P., 'Thermodynamic modelling of the effect of temperature on the hydration and porosity of Portland cement', *Cement and Concrete Research* **38** (1) (2008) 1-18

[11] Ravikumar, D. and Neithalath, N., 'Reaction kinetics in sodium silicate powder and liquid activated slag binders evaluated using isothermal calorimetry', *Thermochimica Acta* **546** (2012) 32-43

[12] Huanhai, Z., Xuequan, W., Zhongzi, X. and Mingshu, T., 'Kinetic study on hydration of alkali-activated slag', *Cement and Concrete Research* **23** (6) (1993) 1253-1258

[13] Shi, C. J. and Day, R. L., 'A Calorimetric Study of Early Hydration of Alkali-Slag Cements', *Cement and Concrete Research* **25** (6) (1995) 1333-1346

[14] Neithalath, N., 'Quantifying the effects of hydration enhancement and dilution in cement pastes containing coarse glass powder', *Journal of Advanced Concrete Technology* **6** (3) (2008) 397-408

[15] Khawam, A. and Flanagan, D. R., 'Solid-state kinetic models: basics and mathematical fundamentals', *The journal of physical chemistry B* **110** (35) (2006) 17315-17328